YALE
PEABODY
MUSEUM

P.O. BOX 208118 | NEW HAVEN CT 06520-8118 USA | PEABODY.YALE. EDU

JOURNAL OF MARINE RESEARCH

The *Journal of Marine Research,* one of the oldest journals in American marine science, published important peer-reviewed original research on a broad array of topics in physical, biological, and chemical oceanography vital to the academic oceanographic community in the long and rich tradition of the Sears Foundation for Marine Research at Yale University.

An archive of all issues from 1937 to 2021 (Volume 1–79) are available through EliScholar, a digital platform for scholarly publishing provided by Yale University Library at https://elischolar.library.yale.edu/.

Requests for permission to clear rights for use of this content should be directed to the authors, their estates, or other representatives. The *Journal of Marine Research* has no contact information beyond the affiliations listed in the published articles. We ask that you provide attribution to the *Journal of Marine Research*.

Yale University provides access to these materials for educational and research purposes only. Copyright or other proprietary rights to content contained in this document may be held by individuals or entities other than, or in addition to, Yale University. You are solely responsible for determining the ownership of the copyright, and for obtaining permission for your intended use. Yale University makes no warranty that your distribution, reproduction, or other use of these materials will not infringe the rights of third parties.

This work is licensed under a Creative Commons Attribution-NonCommercial-ShareAlike 4.0 International License.
https://creativecommons.org/licenses/by-nc-sa/4.0/

Journal of Marine Research, 45, 601–634, 1987

A model for the inertial recirculation of a gyre

by Richard J. Greatbatch[1]

ABSTRACT

This paper considers the "time-mean" circulation of wind-driven ocean gyres in the limit referred to as "inertial" or "almost-free." In this limit, potential vorticity is conserved following the flow with sources and sinks of potential vorticity balancing in an integral sense around the gyre. Approximate analytic solutions are obtained for a continuously stratified quasi-geostrophic ocean by neglecting the relative vorticity in the gyre interiors. The solutions have features similar to those found in the western part of ocean basins both in eddy-resolving numerical models and in observations. In particular, a deep westward recirculation, such as proposed by Worthington (1976) for the Gulf Stream system, arises naturally from the analysis as an enhanced barotropic flow inside the region where the "bowl" containing the circulation has intersected the ocean floor. This flow, which is driven by eddies and dissipated by bottom friction, leads to a sudden increase in westward velocity similar to that found between 35N and 36N in the long-term current records along 55W discussed by Schmitz (1977, 1978, 1980).

1. Introduction

Conservation of potential vorticity, q, provides a basic constraint on motions in the atmosphere and ocean. To break this constraint requires either input of q by means of forcing or its dissipation by frictional processes. In this paper, our concern is with the wind-driven circulation of the ocean and the associated oceanic gyres. In the linear theories of Stommel (1948) and Munk (1950), the forcing and dissipation are assumed to be so effective that a fluid particle moving round the gyre always forgets its q and adjusts to that arising from the planetary rotation at each latitude. Including the nonlinear, inertial terms in the equations of motion allows a fluid particle to have a memory and can lead to radically different dynamics. Indeed the opposite point of view to that implied by linear theory is one in which the effect of forcing and dissipation is so weak that a fluid particle remembers its q throughout many circuits of the gyre so that at lowest order in the dynamics, q is conserved following the motion. The limit in which q is exactly conserved will be referred to as the "inertial," "almost-free" limit.

The realization that inertial effects could be important in the dynamics of ocean gyres arose from attempts to make direct comparisons between linear theory and observations. In the linear models of Stommel (1948) and Munk (1950), there is no net

1. Department of Physics and Newfoundland Institute for Cold Ocean Science, Memorial University of Newfoundland, St. John's, Newfoundland, Canada A1B 3X7.

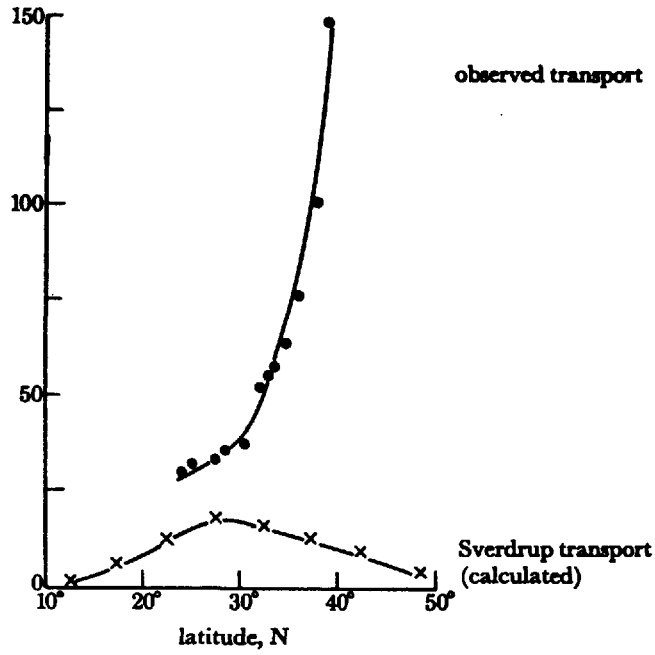

Figure 1. A comparison of the observed Gulf Stream transport (from Knauss (1969)) and the transport according to linear theory, as computed from wind-stress data by Hellerman (1965) (from Gill (1971)).

transport of mass across a latitude circle with the Sverdrup transport farther east being balanced by a narrow, swift, western boundary current. The transport of this current, therefore, depends only on the field of wind stress curl to the east and can be computed from wind data. Figure 1, taken from Gill (1971), shows the calculated and observed transports for the Gulf Stream system as a function of latitude. The observed transport is found to increase with latitude and to be greatly in excess of that predicted by linear theory. It was found, however, that the basic shape of the observed curve could be accounted for by including the neglected nonlinear terms in Stommel's model and solving the problem numerically, as was done by Veronis (1966).

More recent calculations using multi-level, eddy-resolving numerical models (see Holland *et al.* (1983) for a review) also exhibit enhanced transport in the western boundary current like that observed. In these models, the enhanced transport is achieved by means of a deep, eddy-driven recirculation such as can be seen in Figure 2. In the case shown, the model is driven by a symmetric, double-gyre wind stress. The western boundary current leaves the coast at mid-basin to form an eastward jet extending into the interior. This jet is flanked by deep (in fact extending to the ocean floor) eddy-driven westward return flows associated with velocities up to 25 cm sec^{-1} at the surface. A deep, westward recirculation such as this was proposed by Worthington

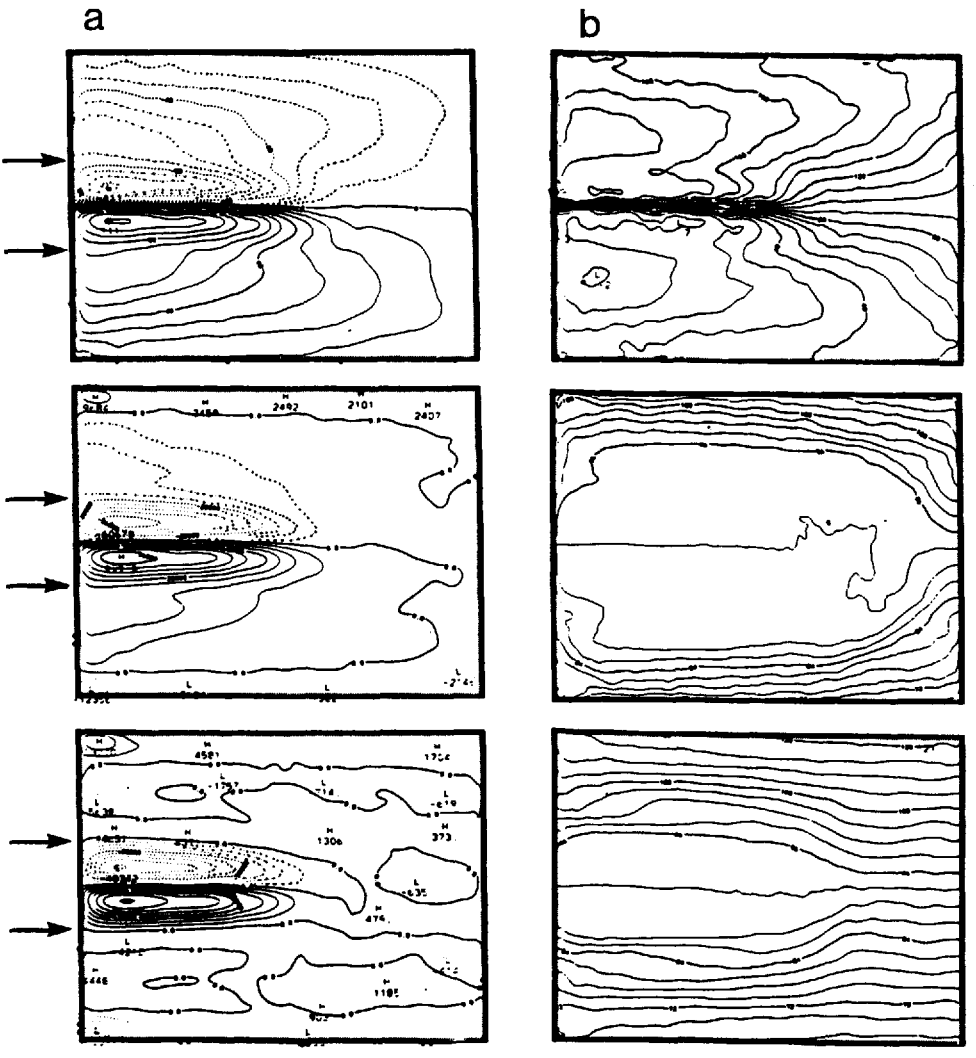

Figure 2. Five year mean streamfunction ψ (Fig. 2a) and potential vorticity q (Fig. 2b) at the top, third and fifth levels, respectively, of an eight level eddy-resolving numerical simulation of the wind-driven circulation, corresponding to mean depths of 150 m, 850 m and 1750 m respectively (from Holland *et al.* (1984)). The arrows mark the boundary of the deep westward recirculation. (Reprinted by permission from Nature, *308*, 698–705. Copyright © 1984 MacMillan Magazines Ltd.)

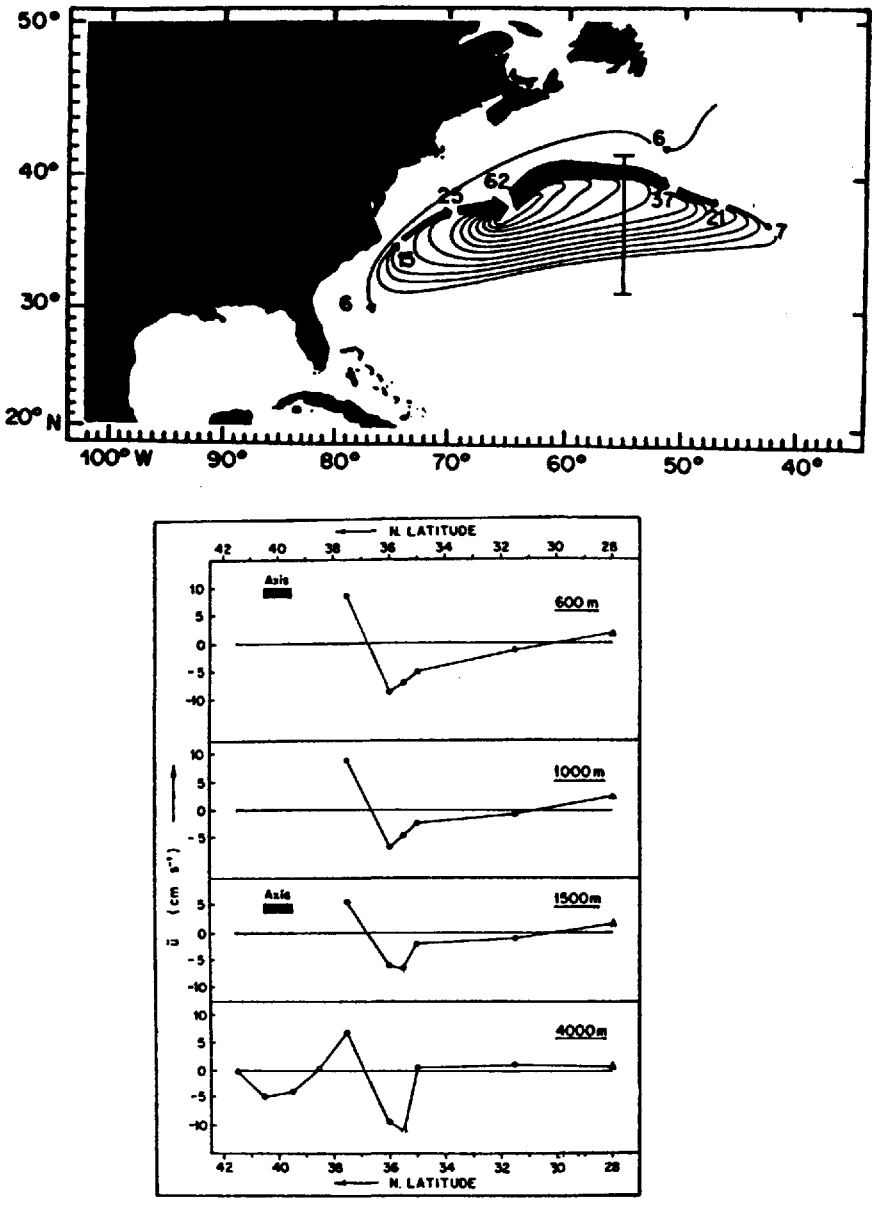

Figure 3. (a) Volume transport streamlines for the deep (potential temperature less than 4°C) general circulation of the North Atlantic according to Worthington (1976). Also shown is the location of the line of moorings along 55W referred to in Figure 3b (from Schmitz, 1977). (b) Time-averaged zonal velocity at locations along 55W at indicated depths (eastward positive). The solid bar is a rough indication of a range of mean positions for the axis of the Gulf Stream (from Schmitz, 1980).

(1976) for the Gulf Stream system (see Fig. 3a). Furthermore, the long-term current records described by Schmitz (1977, 1978, 1980) at locations along 55W show a mean westward flow in Worthington's recirculation area with velocities up to 10 cm sec^{-1} at 4000 m depth (see Fig. 3b). Stommel *et al.* (1978) also found the need for a deep recirculation in order for the Gulf Stream system to maintain an overall mass balance.

In this paper approximate solutions are found which exhibit such a deep recirculation. These are obtained by considering the "inertial," "almost-free" limit. This limit was first utilized by Niiler (1966), who considered wind-driven barotropic ocean circulation, and has recently been suggested by Pierrehumbert and Malguzzi (1984) as a model for blocking in the atmosphere. (Strictly speaking, the idea originates from Batchelor (1956) and is a generalization of the Prandtl-Batchelor theorem in fluid mechanics.) Here we find approximate solutions for a continuously stratified, quasi-geostrophic ocean. The restriction to quasi-geostrophic dynamics is relaxed in Appendix I where a comparison is given between the theory and the hydrographic section along 50W made by *Atlantis* in 1956. The solutions are a generalization of those presented by Marshall and Nurser (1986) who discuss 1½-layer and 2½ layer model oceans. Here, we give a comprehensive theory using continuous stratification and including the interaction with the ocean floor which, as we shall see, is crucial for obtaining a deep, inertial recirculation.

This is not the first paper in which potential vorticity conserving solutions have been sought for a continuously stratified, quasi-geostrophic ocean and suggested as an explanation for the deep transport associated with the Gulf Stream system. Niiler *et al.* (1965) found solutions for which potential vorticity q is a linear function of streamfunction ψ i.e., $q = c_1\psi + c_0$ and compared their solutions with the transport diagram for water lying between 2°C and 12°C that was proposed by Worthington (1965). The coefficients c_1 and c_0 were chosen to be independent of the vertical coordinate z and no attempt was made, as is done here, to relate them to the forcing and dissipation or to take account of the effect of geostrophic eddies about which little was known at that time. Taking account of these factors introduces z-dependence. This plays an important role in our solutions (especially that of c_0 which is crucial for determining the "bowl" which contains the circulation), as discussed in Section 5. The solutions to be presented here are also examples of those discussed by Welander (1971). In particular, the analysis given in Appendix 1 of this paper is an example of his case in which potential vorticity, q, is a function of density alone. Here, however, we have the additional feature of the "bowl" containing the circulation which must be calculated.

The plan of the remainder of this paper is as follows. Section 2 deals with the model geometry and the basic governing equations. In Section 3 the "inertial," "almost-free" limit is described. We are then in a position to write down the equations we actually solve together with the associated boundary conditions. This is done in Section 4. The

structure of the solutions in the interior of the gyres is then considered. The contribution of the relative vorticity in the potential vorticity budget is neglected leading to simple analytical solutions. In Section 5 the structure of the solutions before the circulation has stretched down to the ocean floor is described. Sections 6 and 7 deal with the nature of the solutions once the ocean floor is playing a role. The closure of the circulation by means of inertial boundary currents and an inertial (eastward) jet in the interior of the ocean basin is discussed in Section 8. Solutions for two different choices of the basic density stratification are given in Section 9. Section 10 closes the main body of the paper with a summary and discussion, with particular reference to the influence of the neglected relative vorticity term on the solutions. The paper also includes two appendices. Appendix 1 attempts to compare the theory with the hydrographic section along 50W made by *Atlantis* in 1956. Appendix 2 discusses the appearance of the classical Sverdrup transport as a first order correction to the lowest order flow in the "inertial," "almost-free" limit.

2. The model geometry and governing equations

Figure 4 shows the horizontal and vertical structure of the model ocean (which is flat-bottomed) considered in this paper. We work on a mid-latitude β-plane with cartesian coordinates x, y, z increasing respectively eastward, northward and vertically upward. The model is driven by a symmetrical double-gyre wind stress centered around $y = 0$. We shall think of the two gyre system as being equilibrated by the transfer of potential vorticity between the gyres by geostrophic eddies. The only explicit friction to be considered is bottom friction which will play a role when we consider the deep, eddy-driven recirculation in Section 7.

In this paper, we follow Rhines and Young (1982a) and Young and Rhines (1982) (hereafter referred to as RY and YR respectively) in employing quasi-geostrophic dynamics (some relaxation of this restriction is given in Appendix 1). By so doing, we emphasize the recirculation characteristics of a gyre and exclude the possibility of outcropping and ventilation as described by Luyten *et al.* (1983). Where the model formulation in this paper differs from RY and YR is in the handling of the layer at the surface which is directly acted on by the wind. Here, this layer is itself assumed to be described by quasi-geostrophic dynamics with the Ekman transport due to the wind entering as part of the ageostrophic flow field (this is the approach described by Gill (1982), p. 507). The quasi-geostrophic momentum equations (excluding for the time being the dissipation terms) are then

$$\left.\begin{aligned} f_0 u_a &= \frac{1}{\rho_0 f_0}\left\{\beta y \frac{\partial p'}{\partial y} - \frac{D_g}{Dt}\frac{\partial p'}{\partial x}\right\} + \frac{\tau_y}{\rho_0 H_M} F(z) \\ f_0 v_a &= \frac{1}{\rho_0 f_0}\left\{-\beta y \frac{\partial p'}{\partial x} - \frac{D_g}{Dt}\frac{\partial p'}{\partial y}\right\} - \frac{\tau_x}{\rho_0 H_M} F(z) \end{aligned}\right\} \tag{1}$$

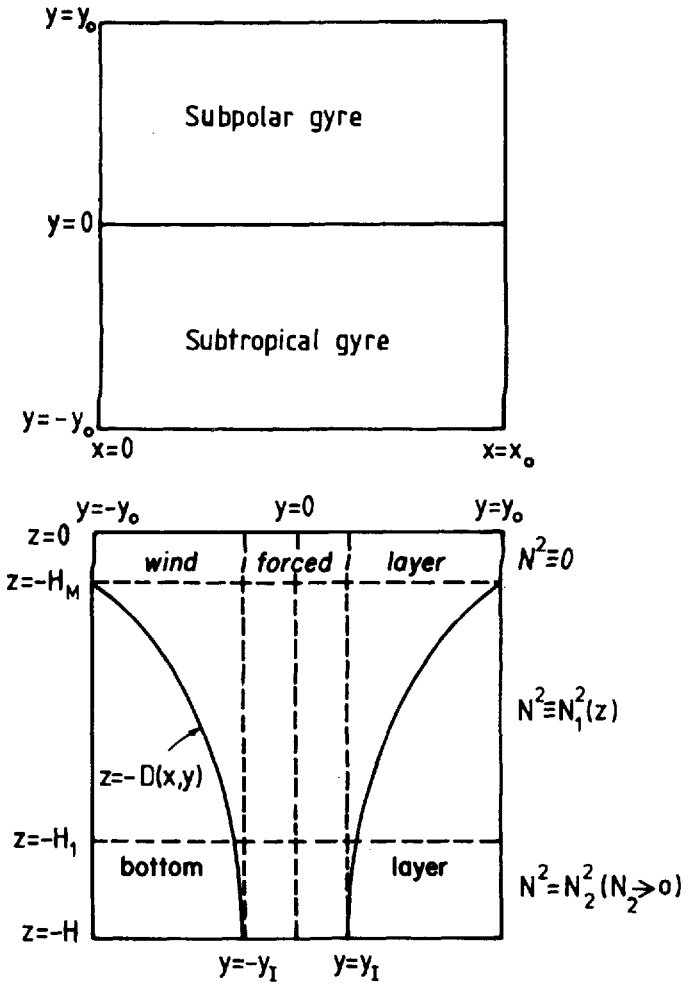

Figure 4. The model geometry. (a) shows a horizontal plan view at the surface and (b) a vertical section across the gyre. The wind stress curl forcing is symmetric about $y = 0$ with positive wind stress curl over the subpolar and negative wind stress curl over the subtropical gyre. $z = -D(x, y)$ marks the edge of the "bowl" containing the circulation.

where

$$F(z) = \begin{cases} 1 & (-H_M \le z \le 0) \\ 0 & (\text{otherwise}) \end{cases}$$

(u_a, v_a) is the ageostrophic velocity field, p' the perturbation pressure, f_0 the value of the Coriolis parameter at $y = 0$, β the gradient of the earth's vorticity, ρ_0 a representative density of sea water and D_g/Dt the rate of change following the

geostrophic flow. The wind forcing $(\tau_x, \tau_y)/\rho_0 H_M$, where (τ_x, τ_y) is the surface stress, is modelled as a body force acting over the layer $-H_M \leq z \leq 0$. H_M is assumed to be independent of x and y. ψ and q will be averaged over this layer and will therefore be taken independent of depth in this layer. We guarantee this by taking the buoyancy frequency N to be zero over this depth range. For convenience the layer $-H_M \leq z \leq 0$ will be referred to as the wind forced layer or WFL for short.

In adopting the quasi-geostrophic formulation, we must also specify a basic density stratification $\bar{\rho}(z)$ which depends only on the vertical coordinate z and is assumed to be fixed in time (we are not concerned here with those mechanisms responsible for maintaining the thermocline which is taken as given). If we take ρ_0 to be the average density, this is equivalent, to specifying the buoyancy frequency N, given by

$$N^2 = -g\bar{\rho}_z/\rho_0 \tag{2}$$

where g is the acceleration due to gravity. In addition to putting $N^2 = 0$ in the WFL, we also assume that there is a layer at the bottom of the ocean, influenced by bottom friction, which is also well-mixed (i.e. $N^2 = 0$). This layer will be referred to as the bottom layer or BL for short. Apart from these layers, however, we do not specify the form of N^2 but allow it to be any physically realizable function of z.

Putting $\sigma = \rho - \bar{\rho}$, where ρ is the total density field, the quasi-geostrophic equation for σ is

$$\frac{D_g\sigma}{Dt} - \rho_0 \frac{N^2 w}{g} = 0 \tag{3}$$

σ is related to the perturbation pressure p' by the hydrostatic relation

$$\frac{\partial p'}{\partial z} = -g\sigma. \tag{4}$$

Combining (1), (3), and (4) with the continuity equation

$$(u_a)_x + (v_a)_y + w_z = 0$$

leads to the governing equation

$$\frac{D_g q}{Dt} = \frac{1}{\rho_0 H_M}\left\{\frac{\partial}{\partial x}(\tau^y) - \frac{\partial}{\partial y}(\tau^x)\right\} F(z) - \mathcal{D}, \tag{5}$$

$$\text{where} \quad q = \nabla^2\psi + \beta y + \frac{\partial}{\partial z}\left\{\frac{f_0^2}{N^2}\frac{\partial \psi}{\partial z}\right\}$$

is the quasi-geostrophic potential vorticity, $\psi = p'/(f_0\rho_0)$ is the quasi-geostrophic streamfunction, and $\mathcal{D}$ represents the dissipation. In this paper, we are concerned with the steady, "time-mean" circulation obtained by time averaging (5). This leads to

$$J(\psi, q) = \mathcal{F} - \mathcal{D} - \nabla \cdot (\overline{u'q'}) \tag{6}$$

where J is the Jacobian operator, $\mathcal{F}$ represents the wind forcing and $\nabla \cdot (\overline{u'q'})$ is the eddy flux divergence term.

Eq. (6) is the fundamental equation we shall be concerned with. Throughout, we shall parameterise the eddy-flux divergence term as a downgradient transfer of q by eddies so that

$$-\nabla \cdot (\overline{u'q'}) = \nabla \cdot (K \nabla q) \tag{7}$$

for some $K > 0$ which will depend on the spatial coordinates x, y, z (it should be noted that the divergence and gradient operators in (6) and (7) denote the horizontal divergence and gradient only). For justification of this the reader is referred to Rhines and Holland (1979) and Marshall and Shutts (1981).

As we shall see, the most important part of the problem is to calculate the "bowl" whose edge is defined by $z = -D(x, y)$ and which contains the circulation. This feature also formed part of the model formulation in RY and YR. As described by them, inside the "bowl" the q contours are closed enabling the "weak" eddy forcing to generate strong currents. Outside, the q contours intersect the boundaries so that "weak" eddy forcing can only generate weak currents. We therefore identify the region $z \geq -D$ as being the region occupied by the circulation and assume that outside this region the ocean is at rest.

3. The "inertial," "almost-free" limit

We now consider the mathematical basis for the "inertial," "almost-free" limit. Readers are referred to the papers by Niiler (1966), Pierrehumbert and Malguzzi (1984) (hereafter referred to as PM) and Marshall and Nurser (1986) for further discussion.

Following PM, we write the governing equation for the "time-mean" circulation as

$$J(\psi, q) = \epsilon G \tag{8}$$

where the term ϵG represents the forcing (i.e. wind stress curl), the dissipation and the eddy-flux divergence of q. As in PM, we assume that the dimensionless parameter $\epsilon \ll 1$. Niiler (1966) showed that for a barotropic ocean, ϵ is the ratio of the velocity associated with the Sverdrup transport in the interior of the ocean to that associated with the free, inertial solution of (9) (see below) which is assumed to dominate the flow. This is true here also. In fact, although the Sverdrup constraint does not enter into the lowest order dynamics considered here, it does enter at next order as described in Appendix 2.

Following PM, we expand ψ, q and G in powers of ϵ

$$\psi = \psi_0 + \epsilon\psi_1 + \ldots$$
$$q = q_0 + \epsilon q_1 + \ldots$$
$$G = G_0 + \epsilon G_1 + \ldots$$

and substitute these expansions into the governing equation (8). At lowest order, that is matching terms of $0(\epsilon^0)$, we obtain

$$J(\psi_0, q_0) = 0 \tag{9}$$

of which the general solution is

$$q_0 = Q(\psi_0, z). \tag{10}$$

At this stage, Q is an arbitrary function. By considering what happens at next order, and so taking account of the term ϵG, the variation of Q between ψ_0 streamlines is determined. Q is then a known function of ψ_0 and z up to a z-dependent constant which can be determined. The problem then becomes one of solving (10) for the streamfunction ψ_0.

Matching terms of order ϵ^1 in the expansion of (8) gives

$$J(\psi_0, q_1) + J(\psi_1, q_0) = G_0 \tag{11}$$

which, following PM, can be written as

$$J\left(\psi_0, q_1 - \frac{\partial Q}{\partial \psi_0}(\psi_0, z)\psi_1\right) = G_0. \tag{12}$$

Integrating (12) over the area enclosed by any closed ψ_0 streamline in a horizontal plane leads to the constraint

$$\int G_0 dA = 0 \tag{13}$$

(The reason for calling the limit $\epsilon \ll 1$ "almost-free" is that although the lowest order flow given by (10) is potential vorticity conserving, it still knows about sources and sinks of potential vorticity through (13).)

Marshall and Nurser (1986) have shown that when wind stress curl forcing is being balanced by down-gradient transfer of q by eddies, as is the case in the WFL in our model, then $\partial Q/\partial \psi_0$ is required by (13) to be negative. To see this, note that since

$$\epsilon G_0 = \frac{\hat{k} \cdot \nabla x \tau}{\rho_0 H_M} + \nabla \cdot (K \nabla q_0)$$

it follows from (13) that

$$\frac{1}{\rho_0 H_M} \int_A \hat{k} \cdot \nabla x \tau dA = - \int_A \nabla \cdot (K \nabla q_0) dA \tag{14}$$

which using Stoke's theorem on the left-hand side and Gauss' Divergence Theorem on the right hand side leads to

$$\frac{1}{\rho_0 H_M} \oint \tau \cdot dl = - \oint K \nabla q_0 \cdot \hat{n} dl$$

where here the integrals are around the closed ψ_0 streamline enclosing the area A and $\hat{\boldsymbol{n}}$ is an outward unit vector normal to this streamline. Substituting for q_0 from (10) we then conclude that

$$\frac{\partial Q}{\partial \psi_0}(\psi_0, z) = -\frac{1}{\rho_0 H_M} \oint \boldsymbol{\tau} \cdot d\boldsymbol{l} \Big/ \oint K\boldsymbol{u} \cdot d\boldsymbol{l}. \tag{15}$$

This shows that where the wind stress $\boldsymbol{\tau}$ and the ocean currents circulate in the same sense (as they do in the ocean) then $\partial Q/\partial \psi_0 < 0$. Marshall and Nurser (1986) give a simple physical interpretation of this result: basically if we have a subtropical gyre, for example, for which ψ_0 increases into the interior of the gyre, the only way down-gradient transfer of q can balance the wind-stress curl forcing, which is tending to decrease q in the gyre interior, is for $\partial Q/\partial \psi_0 < 0$.

By a similar argument, we can show that if down-gradient transfer of q by eddies is being balanced by dissipation of vorticity by bottom friction (as is the case in the BL) so that

$$\epsilon G_0 = \nabla \cdot (K \nabla q_0) - \gamma \nabla^2 \psi_0$$

where γ is the (assumed) spatially uniform bottom friction coefficient, then (13) implies that

$$\frac{\partial Q}{\partial \psi_0} = \gamma \oint \boldsymbol{u} \cdot d\boldsymbol{l} \Big/ \oint K\boldsymbol{u} \cdot d\boldsymbol{l}. \tag{16}$$

so that now $\partial Q/\partial \psi_0$ is positive. In each case, the integral constraint (13) has fixed the gradient of Q with respect to streamfunction ψ_0 at each level z. When the only mechanism available for influencing q is downgradient transfer by eddies, as in those regions of a gyre isolated from both surface forcing and bottom friction, then

$$\partial Q/\partial \psi_0 = 0 \tag{17}$$

as can be seen by putting $\boldsymbol{\tau} = \boldsymbol{0}$ in (15) or $\gamma = 0$ in (16). This is the result obtained by Rhines and Young (1982b) implying homogenization of potential vorticity along isopycnal surfaces in such regions.

Keffer (1985) has recently published maps of the potential vorticity field on isopycnal surfaces (which in the quasi-geostrophic formulation used here are just the horizontal planes z = constant). Of particular interest are Keffer's Figures 11 and 15 for the Pacific Ocean. These show regions of homogenized potential vorticity on isopycnal surfaces isolated from surface forcing. Also Keffer's Figures 4 and 5 show potential vorticity decreasing into the interior of the subtropical gyres in both the Atlantic and Pacific Oceans on isopycnal surfaces directly affected by surface forcing. These features are in agreement with the general prediction of Eqs. (15) and (17) and are also exhibited by the eddy-resolving numerical model shown in Figure 2.

4. The equations to be solved

We now describe the equations to be solved and the associated boundary conditions. We seek solutions which apply in the "inertial," "almost-free" limit. This means that at lowest order

$$q = Q(\psi, z) \tag{18}$$

for some function Q (cf. Eq. (10)), where now the subscript 0 on q and ψ is dropped. In this paper, we restrict Q to be linear in ψ at each z. The presence of eddies, represented by the diffusion coefficient K, does provide some flexibility in Eqs. (15) and (16) whereby the eddies could conceivably arrange themselves in some "maximum entropy" state in which the q-ψ relationship is indeed linear. There is some evidence for this from eddy-resolving numerical models (e.g. Rhines *et al.* (1985), McWilliams *et al.* (1978) who consider a channel model—see their Figs. 25 and 26—and Bretherton and Haidvogel (1976)). Basically, however, this simplification must be judged by the success of the solutions in describing features of the observed ocean circulation, on the one hand, and eddy-resolving numerical models on the other.

The problem is now to solve

$$q \equiv \nabla^2\psi + \beta y + \frac{\partial}{\partial z}\left\{\frac{f_0^2}{N^2}\frac{\partial \psi}{\partial z}\right\} = c_1(z)\psi + c_0(z) \tag{19}$$

for $z \geq -D(x, y)$ with appropriate choice of $c_1(z)$ and $c_0(z)$. As already discussed at the end of Section 2, part of the problem is to solve for the surface $z = -D$ which bounds the circulation. For $z < -D$ the ocean is at rest and $q = \beta y$.

We choose $c_1(z)$ consistent with the integral constraint (13). We shall therefore solve (19) with $c_1(z)$ given by

$$c_1(z) = \begin{cases} -A^2 & (-H_M \leq z \leq 0) \\ 0 & (-H_1 < z < -H_M) \\ B^2 & (-H \leq z \leq -H_1) \end{cases} \tag{20}$$

where A and B are real constants so that $c_1 < 0$ in the WFL (as required by (15)), $c_1 = 0$ in the region $-H_1 < z < H_M$ (as required by (17)) and $c_1 > 0$ in the BL (as required by (16)).

For $c_0(z)$ we take

$$c_0(z) = \begin{cases} \beta y_0 & (-H_M \leq z \leq 0, \quad y > 0) \\ -\beta y_0 & (-H_M \leq z \leq 0, \quad y < 0) \\ 0 & (\text{otherwise}). \end{cases} \tag{21}$$

This is the choice made by Marshall and Nurser (1986) for their calculations and is consistent both with eddy-resolving numerical models and with observations. In the

WFL there is a discontinuity in q along $y = 0$. This corresponds to the sharp gradient in q found in the top-most level of the numerical model shown in Figure 2. This occurs where the eastward jet penetrates from the western boundary into the ocean interior. It corresponds, in the observations of Bower *et al.* (1985) to the appearance of the Gulf Stream as a "barrier" to the transfer of q in those layers strongly influenced by surface forcing.

Putting $c_0(z) = 0$ in the region $z < -H_M$ implies, where $c_1(z)$ is also zero, homogenization of q across both gyres to the same value. This is found in numerical models (see those levels in Figure 2 at depths of 850 m and 1750 m) and corresponds to the "blender" effect found by Bower *et al.* (1985) in those layers isolated from the surface. Figure 11 in Keffer (1985) also suggests this kind of behavior in the Pacific Ocean.

We shall see in the next section of this paper that the disparity in the value of $c_0(z)$ between the surface layer exposed to the wind and the region beneath is crucial to the solutions we obtain. We defer until then a discussion of the dynamical reasons for choosing $c_0(z)$ as in (21).

We now turn to the boundary conditions under which (19) is to be solved. The condition of no normal velocity along the edge of the basin implies

$$\psi = 0 \quad \text{along } y = \pm y_0 \quad \text{and } x = 0, \quad x = x_0. \tag{22}$$

We also have,

$$\psi = 0 \quad \text{along } y = 0. \tag{23}$$

Along the edge of the "bowl" $z = -D(x, y)$ we have

$$\left.\begin{aligned} \psi &= 0 \\ -\frac{f_0}{N^2}\psi_z &= 0 \end{aligned}\right\} \quad \text{along } z = -D(x, y) \tag{24}$$

which ensures continuity of pressure and isopycnal displacement, respectively, across $z = -D$. It is possible that the "bowl" will intersect the ocean floor at $z = -H$ in which case (24) is replaced by

$$-\frac{f_0}{N^2}\psi_z = 0 \quad \text{at } z = -H. \tag{25}$$

We also have

$$-\frac{f_0}{N^2}\psi_z = 0 \quad \text{at } z = 0. \tag{26}$$

(If the ocean is spun up from rest, then (25) and (26) are a consequence of assuming that the vertical velocity $w = 0$ at $z = -H$ and $z = 0$ for all time.)

5. The flow in the gyre interiors

The prototype potential vorticity conserving solution on which those in this paper are built is that of Fofonoff (1954) shown in Figure 5. This solution is for a barotropic ocean and consists of a broad westward flow in the gyre interior, where the relative vorticity $\nabla^2\psi$ can be neglected in the potential vorticity budget, and narrow inertial jets which close the circulation. We seek solutions of a similar form here and begin by neglecting $\nabla^2\psi$ in (19). In Section 8, this term is restored when we consider the inertial jets that close the circulation and in Section 10 a discussion is given on how we expect this term to modify the solutions found here.

Let us therefore begin by seeking the solution for the gyre interiors. In this section we consider only that part of the solution for which D, the depth of the circulation, is less than H_1. The effect of the BL is treated in Section 7. Note also that throughout this paper, solutions will be found only for the subtropical gyre. The corresponding part of the solution for the subpolar gyre can be found by replacing y_0 by $-y_0$ throughout. This exact symmetry is a feature of quasi-geostrophic dynamics.

In the region $-H_1 < z < -H_M$, (19) becomes, neglecting $\nabla^2\psi$

$$\beta y + \frac{\partial}{\partial z}\left\{\frac{f_0^2}{N^2}\frac{\partial \psi}{\partial z}\right\} = 0. \tag{27}$$

Integrating (27) using the lower boundary conditions (24) gives an expression for the isopycnal displacement

$$-\frac{f_0}{N^2}\frac{\partial \psi}{\partial z} = \frac{\beta y}{f_0}(z + D) \tag{28}$$

and the streamfunction ψ

$$\psi = -\frac{\beta y}{f_0^2}\int_{-D}^{z} N^2(z + D)dz. \tag{29}$$

Within the layer $-H_M \leq z \leq 0$ where $N^2 = 0$, ψ is independent of z and must be given by (29) evaluated at $z = -H_M$ to ensure continuity of pressure across $z = -H_M$. It follows that the entire solution is known once we know D, the depth to which the circulation penetrates.

To determine D account must be taken of the dynamics in the WFL. To see this, we note that the potential vorticity q_M, of that layer is given by (neglecting the relative vorticity)

$$q_M = \beta y + \frac{f_0 h}{H_M} \tag{30}$$

where h is the displacement of the isopycnal at the base of the layer and (26) has been used. Continuity of isopycnal displacement across $z = -H_M$ requires h to be given by

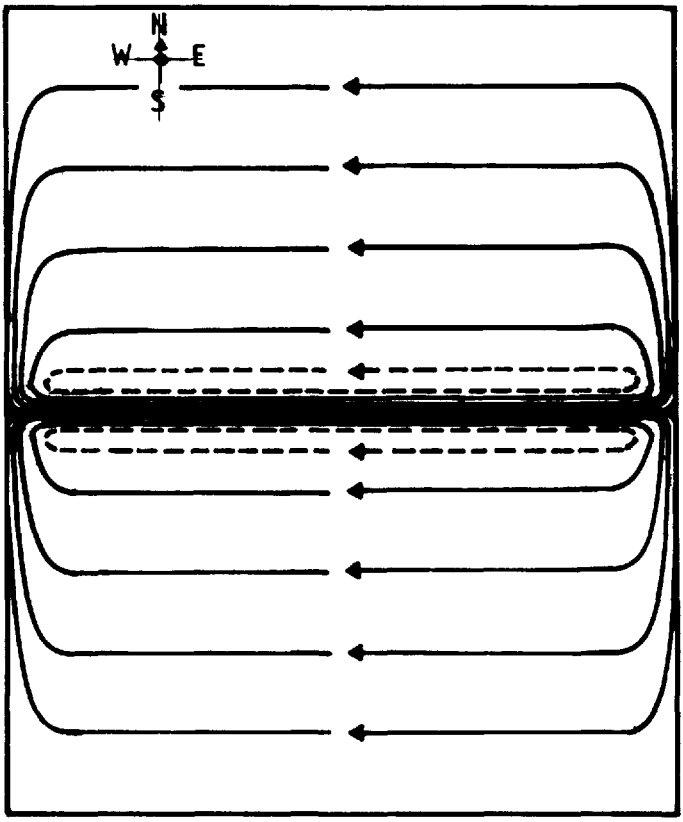

Figure 5. Streamlines ψ = constant for the solution found by Fofonoff (1954).

(28) evaluated at $z = -H_M$ i.e.

$$h = \frac{\beta y}{f_0}(D - H_M). \tag{31}$$

Combining (30) and (31) gives

$$q_M = \beta y D / H_M \tag{32}$$

which directly relates q_M and D.

For our problem, q_M is given by (cf. (19))

$$q_M = -A^2 \psi_M - \beta y_0 \tag{33}$$

where use has been made of (20) and (21) to give c_1 and c_0 and ψ_M refers to the streamfunction ψ evaluated in the WFL. Substituting into (32) gives

$$D = -\frac{H_M y_0}{y} - \frac{A^2 H_M}{\beta y}\psi_M. \tag{34}$$

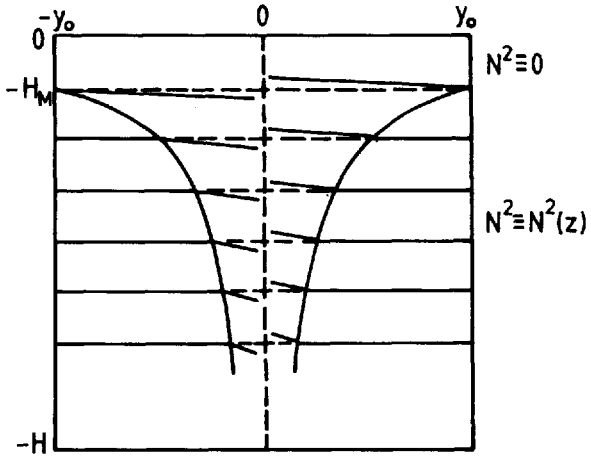

Figure 6. A vertical section showing the isopycnal displacements when $A^2 = 0$ and $\beta y_0/f_0 = 0.2$. Also shown is the edge of the "bowl" containing circulation defined by $z = -D$.

The associated isopycnal displacements are then obtained by substituting this D into (28) i.e.

$$-\frac{f_0}{N^2}\frac{\partial \psi}{\partial z} = \frac{\beta}{f_0}\left\{yz - H_M y_0 - \frac{A^2 H_M \psi_M}{\beta}\right\} \quad (z \leq -H_M) \tag{35}$$

Figure 6 shows D and the associated isopycnal displacements when $A^2 = 0$. This is used as a reference case in the discussion to follow.

Eq. (34) has a simple physical interpretation. The boundary conditions (24) and (26) imply that there can be no net vortex stretching in any vertical column of fluid (indeed (34) can be obtained by integrating (19), with the $\nabla^2\psi$ term neglected, between $z = 0$ and $z = -D$, using (24) and (26) to eliminate the stretching term and dividing the result by βy). Let us begin by considering what this means for the subtropical gyre; that is the region $-y_0 \leq y < 0$ in which $\psi_M \geq 0$. Substituting for q_M from (33) into (30) gives

$$h = -\frac{H_M}{f_0}\{A^2\psi_M + \beta(y_0 + y)\}. \tag{36}$$

It follows that the isopycnal at the base of the WFL is displaced increasingly downward as we move northward from the southern boundary of the gyre at $y = -y_0$. This can be seen in Figure 6. On the other hand, isopycnals below the WFL, where $q = 0$, are increasingly squashed as we move southward from $y = 0$. In this way, the vortex stretching in the WFL is compensated by vortex squashing below, the depth of penetration of the circulation D being precisely that depth at which the net vortex stretching in the column is zero. Furthermore, the larger $A^2 > 0$, the more the WFL is

stretched and the greater becomes the depth required for the net vortex stretching to be zero. Note also that the nearer we are to $y = 0$ the greater is the stretching in the WFL but the less is the squashing below. This forces D to deepen rapidly as we move toward $y = 0$ (as in Fig. 6). For the subpolar gyre the situation is reversed. Here, vortex squashing in the WFL is compensated by vortex stretching below and the depth D is once again the depth at which the net vortex stretching is zero.

The crucial factor which enables the above argument to work is the disparity between the value of the coefficient c_0 (cf. (21)) in the WFL and its value in the region below. The effect of c_0 is to select the latitude at which isopycnals have the same spacing as in the basic stratification (see discussion leading to Eq. (2)), corresponding to a state of zero vortex stretching. For the case of the subtropical (subpolar) gyre this latitude is the southern (northern) boundary of the gyre in the WFL, but is at mid-basin $y = 0$ below.

Let us now consider the dynamics which leads to this choice for c_0. Putting $c_0(z) = 0$ in the region $z \leq -H_M$ follows directly from the argument by Marshall and Nurser (1986) for the appearance of closed contours in the lower active layer of their $2\frac{1}{2}$ layer model. This is because the outer of their closed contours is that corresponding to $q = 0$. To obtain the continuously stratified case considered here we simply consider the limit in which the number of layers and the vertical resolution are progressively increased (this is the same argument as given by RY for their "choice of Y"—see p. 581 and Fig. 8 in their paper). The choice for $c_0(z)$ in the WFL can be understood by considering the spin-up of an ocean from a state of rest following the application of wind forcing. Initially we develop a Sverdrup regime away from the western boundary. In this region fluid particles have their potential vorticity adjusted as they move outward from $y = 0$ by the action of the surface wind stress curl. This flow is returned by western boundary currents which become increasingly nonlinear and carry the potential vorticity $\pm\beta y_0$ at the northern and southern boundaries of the gyres toward $y = 0$. Here the discontinuity in q implied by (21) and which can be seen in Figure 2 develops. In this way the value for c_0 appropriate to the WFL is selected by the disparity between the Sverdrup region on the one hand, where essentially linear dynamics apply, and the highly nonlinear, swift, western boundary current on the other which is the key to setting up the "inertial" solutions described here.

Let us now examine the isopycnal displacements in more detail. These are given by (35). Figure 6 shows these displacements when $A^2 = 0$. In this case

$$\frac{-f_0}{N^2}\frac{\partial \psi}{\partial z} = \frac{\beta}{f_0}(yz - y_0 H_M)$$

so that the isopycnal displacements at each z are just straight lines sloping downward in the subtropical gyre and upward in the subpolar gyre, as shown. This is similar to the slope of isopycnals found from hydrographic sections across the recirculation area of the Gulf Stream see, for example, Figure 8 and also the sections discussed by

McDowell *et al.* (1982). Note that when $A^2 > 0$, the slope of the isopycnals is increased (and increases toward $y = 0$) in response to the increased pushing down (subtropical gyre)/pulling up (subpolar gyre) of the isopycnal at the base of the WFL (see (36)).

We now turn to the velocity field which is obtained by differentiating (29) with respect to x and y and using (34) to give D. Since D is independent of x in the gyre interiors, the flow is entirely zonal and is given by

$$u \equiv -\psi_y = \frac{\beta}{f_0^2}\int_{-D}^{z} N^2\left\{z + \frac{A^2 U H_M}{\beta}\right\} dz \tag{37}$$

where $U = -\psi_{My}$ is the velocity in the WFL. We shall see in Section 8 that in order to close the gyres by inertial boundary layers we must have westward flow in the gyre interiors i.e. $u < 0$. (See also Pedlosky (1965) and Robinson (1965)). Since $z < 0$, this is clearly guaranteed by (37) if U is also westward. Evaluating (37) at $z = -H_M$ gives the following expression for U

$$U\left\{1 - \frac{A^2 H_M}{f_0^2}\int_{-D}^{-H_M} N^2\, dz\right\} = \frac{\beta}{f_0^2}\int_{-D}^{-H_M} N^2 z\, dz \tag{38}$$

Westward flow is therefore guaranteed if the parameter $\alpha < 1$ where

$$\alpha = \frac{A^2 H_M}{f_0^2}\int_{-H}^{-H_M} N^2\, dz \tag{39}$$

and H is the total depth of the ocean. The results can be interpreted physically by noting that the velocity field (37) could have been obtained by integrating the thermal wind relation upward from the edge of the "bowl" $z = -D$, which is a surface of no motion, using the known density field. The slope of the isopycnals shown in Figure 6 (which is for $A^2 = 0$) clearly implies flow which increases westward with height since in both gyres, subtropical and subpolar, density decreases northward on each horizontal plane. As A^2 increases from 0, the slope of the isopycnals increases and hence also the horizontal density gradients implying swifter currents as predicted by (37) (since $U < 0$). If A^2 becomes sufficiently large (i.e. $\alpha \to 1$) then the horizontal density gradients become so large that the surface flow increases indefinitely and ultimately will reverse ($\alpha > 1$).

Let us now consider the magnitude of the currents that can be accommodated by (37). Clearly the maximum current, U_{MAX}, obtainable for any given value of A (such that $\alpha < 1$), is given by taking $z = -H_M$ and $D = H$, the total depth of the ocean. It follows that

$$U_{MAX} = \frac{1}{(1-\alpha)}\frac{\beta}{f_0^2}\int_{-H}^{-H_M} N^2 z\, dz \tag{40}$$

When $\alpha = 0$, this is essentially the propagation speed for baroclinic, long Rossby waves

and is only of order 5 cm sec^{-1}. For the model shown in Figure 2 velocities up to 25 cm sec^{-1} are found in the westward recirculation areas that flank the eastward interior jet. Clearly, velocities of this magnitude could be accounted for if A^2 is sufficiently large i.e. α sufficiently near 1. These velocities, however, are occurring in a region where the "time-mean" flow in the model extends to the ocean floor (personal communication, W.R. Holland) and a more likely explanation of their magnitude can be given by taking account of this fact as is done in Section 7.

Before leaving this section, it should be noted that the magnitude of the westward velocity given by (37) increases as we approach $y = 0$ and it is possible, especially in cases for which α is near 1, that it is no longer consistent to neglect the relative vorticity *term $\nabla^2\psi$ in the potential vorticity budget (This is discussed further in Section 10).* This increase in velocity, which is due to the increasing depth of penetration D of the gyre, was also found by Marshall and Nurser (1986) in their 2½ layer calculation. There, the velocity in the upper of their two active layers exhibits a discontinuous jump at the latitude marking the edge of the gyre in the lower layer. This discontinuity is a consequence of the poor vertical resolution in their model and is reproduced here by taking N^2 in (37) to be a sum of two delta functions corresponding to the discrete stratification implied by the layered formulation. When N^2 is a continuous function of depth z, the velocity u varies continuously with latitude y.

6. The intersection of the "bowl" with the ocean floor

In this and the next section we shall consider the influence of the ocean floor and the associated bottom layer on the solutions found in Section 5. We begin by considering the latitude $y = \pm y_I$ at which the "bowl" containing the circulation intersects the floor, and the dependence of this latitude on the structure of the basic stratification (for the model geometry, see Fig. 4).

As noted in Section 2, we assume that the BL is well-mixed i.e. $N^2 = 0$ there. As for the WFL this ensures that the streamfunction ψ is independent of z in that layer. It also has the advantage that until the "bowl" actually meets the ocean floor, $\psi = 0$ in the BL and the full solution is that already discussed in Section 5. In particular, the depth D to which the circulation penetrates is still given by (34) so to find y_I we simply put $D = H$ in (34) and solve for y.

This gives

$$y_I = H_M y_0 \Big/ \left\{(1 - \alpha)H - \frac{A^2 H_M}{f_0^2} \int_{-H}^{-H_M} zN^2\, dz\right\}. \tag{41}$$

When $\alpha = 0$ (i.e. $A^2 = 0$), y_I is independent of N and so does not depend on the basic stratification. To illustrate the behavior of y_I for $\alpha > 0$, let us consider an ocean for

which N has a uniform value N_1 over the depth range $-H_1 < z < -H_M$ and is zero otherwise i.e.

$$N = \begin{cases} 0 & (-H_M \leq z \leq 0) \\ N_1 & (-H_1 < z < -H_M) \\ 0 & (-H \leq z \leq -H_1) \end{cases} \tag{42}$$

in which case (41) becomes

$$y_I = H_M y_0 \Big/ \left\{(1 - \alpha)H + \frac{\alpha}{2}(H_M + H_1)\right\}. \tag{43}$$

It is easy to show that as α increases, the latitude y_I moves farther away from $y = 0$ (this is a general result and can be shown from (41)). In the extreme case $\alpha = 1$,

$$y_I = 2H_M y_0/(H_M + H_1).$$

It follows that when N is given by (42), y_I always lies in the range

$$\frac{H_M y_0}{H} \leq y_I \leq \frac{2H_M y_0}{(H_M + H_1)}. \tag{44}$$

Note that as the stratification is confined into a progressively thinner region immediately below the WFL i.e. as $H_1 \to H_M$, $2H_M y_0/(H_M + H_1) \to y_0$. It is clear, therefore, that if the thermocline is sharp and α is near to 1 then the ocean floor can be expected to have a big influence on the solution. As discussed in Section 10, the influence of the neglected relative vorticity terms is also likely to increase the area in which the presence of the ocean floor is felt.

7. The effect of the ocean floor

Once the "bowl" has intersected the ocean floor, the lower boundary condition (24) is replaced by (25). This means that whereas if the ocean were infinitely deep the isopycnal displacement would be brought to zero at depth D as given by (34), it must now be brought to zero at the ocean floor which is at depth $H < D$. In order to achieve this, the barotropic circulation of the gyre is enhanced. We can see this by integrating (19) (with the relative vorticity term neglected) between the top and bottom of the ocean using (25) and (26) to give

$$H\beta y = -A^2\psi_M H_M + B^2\psi_B(H - H_1) - H_M\beta y_0. \tag{45}$$

Here c_0 has been chosen appropriate to the subtropical gyre (subpolar gyre obtained by replacing y_0 by $-y_0$) and ψ_M and ψ_B are the streamfunctions in the WFL and BL, respectively, both independent of z. Defining D to be as given by (34), (45) can be

written as

$$(D - H)\beta y = -B^2\psi_B(H - H_1) \tag{46}$$

from which we can see that since $D > H$, ψ_B is nonzero.

Now above the BL, the isopycnal displacements can be obtained by integrating (19) (with $\nabla^2\psi$ neglected) down from the surface $z = 0$ using Eq. (26). This means that they are given by the same formula as they were in Section (5) i.e. (28) with D given by (34). Above the BL, therefore, the baroclinic structure of the gyre is governed in the same way as it would be in an infinitely deep ocean, and the streamfunction ψ is given by (29) but now with an additional barotropic component ψ_B given by (46) i.e.

$$\psi = -\frac{\beta y}{f_0^2}\int_{-D}^{z} N^2(z + D)\,dz - \frac{(D - H)\beta y}{B^2(H - H_1)} \tag{47}$$

where D is given by (34) (actually, since $N^2 = 0$ in both the WFL and the BL, (47) holds at all depths and, furthermore, the integral can be taken from depth H rather than D). The velocity (which has no meridional component) is now obtained by differentiating (47) with respect to y

$$u \equiv -\psi_y = \frac{\beta}{f_0^2}\int_{-H}^{z} N^2\left(z + \frac{A^2UH_M}{\beta}\right)dz - \frac{\beta}{B^2(H - H_1)}\left\{H - \frac{A^2H_MU}{\beta}\right\}. \tag{48}$$

The enhanced barotropic circulation is now clearly revealed by comparing (48) with Eq. (37).

To obtain the velocity U we put $z = -H_M$ in (48). The resulting equation can then be rearranged to give

$$U\left\{1 - \alpha - \frac{A^2H_M}{B^2(H - H_1)}\right\} = \frac{\beta}{f_0^2}\int_{-H}^{-H_M} N^2z\,dz - \frac{\beta H}{B^2(H - H_1)} \tag{49}$$

which is a generalization of (38). This time, in order to ensure westward flow, we must have

$$1 - \alpha - \frac{A^2H_M}{B^2(H - H_1)} > 0. \tag{50}$$

An interesting feature of (49) is the inverse dependence of U (and also ψ_B in (46)) on B^2. This means that the more efficient eddies are in smoothing out gradients of q in the BL (recall that $B^2 = \partial q/\partial\psi$) the swifter is the resulting circulation (see, however, the discussion in Section 10 regarding the neglected relative vorticity term). This clearly reveals the role of eddies in driving the enhanced barotropic circulation against the dissipative effects of bottom friction. It is easy to understand how this inverse

dependence arises. We have seen that above the BL, the baroclinic structure of the gyre is governed in the same way that it would be an infinitely deep ocean. The displacement of the isopycnal at the top of the BL is part of this baroclinic structure and therefore imposes the gradient $\partial q/\partial y$ of potential vorticity that is experienced by the BL. Since $\partial q/\partial y = \partial q/\partial \psi \cdot \partial \psi/\partial y$ i.e. $\partial q/\partial y = -B^2 \cdot u$, the inverse dependence of u on B^2 is immediately apparent.

8. The inertial jets that close the circulation

In this section we show how the circulation in the gyre interiors discussed in Sections 5 and 7 can be closed by inertial jets along the western and eastern boundaries and along $y = 0$ provided the interior flow is westward (as found by Pedlosky (1965) and Robinson (1965)).

Let us begin by differentiating (19) with respect to y so that within the "bowl" we have

$$\nabla^2 u + \frac{\partial}{\partial z}\left\{\frac{f_0^2}{N^2}\frac{\partial u}{\partial z}\right\} = c_1(z)u + \beta \tag{51}$$

where $u = -\psi_y$ is the zonal velocity measured positive eastward. The solutions we have found so far in this paper have been obtained by neglecting the ∇^2 term in (51).

Denoting these solutions by u_I, they satisfy

$$\frac{\partial}{\partial z}\left\{\frac{f_0^2}{N^2}\frac{\partial u_I}{\partial z}\right\} = c_1(z)u_I + \beta. \tag{52}$$

We now seek solutions to (51) of the form $u = \phi(x, y, z)u_I(y, z)$. Substituting this expression for u into (51), neglecting the term involving $\nabla^2 u_I$ and using (52), gives

$$\nabla^2\phi + \frac{\partial}{\partial z}\left\{\frac{f_0^2}{N^2}\frac{\partial \phi}{\partial z}\right\} + \frac{\beta}{u_I}\phi = \frac{\beta}{u_I} - 2\left\{\nabla u_I \cdot \nabla\phi + \phi_z u_{I_z}\frac{f_0^2}{N^2}\right\} \tag{53}$$

from which it is clear that provided $u_I < 0$, i.e. the interior flow is westward, ϕ has exponential behavior and the circulation can be closed as required. Furthermore, the boundary layer on the western and eastern boundaries will have local width $(-u_I/\beta)^{1/2}$, which is the standard width for an inertial boundary layer, and the jet along $y = 0$ will have half-width $(-u_I/\beta)^{1/2}$ where here u_I is evaluated at $y = 0$. These statements assume that ϕ varies across the boundary current and eastward jet faster than the scale of variation of u_I.

These conclusions have been reached without actually stating the boundary conditions under which (51) must be solved. These come from (22) and (23). Along the western and eastern boundaries we have $\phi = 0$ which ensures no normal velocity there. The condition on ϕ at $y = 0$ comes from ensuring that all the mass associated with the westward interior flow is returned by the eastward jet.

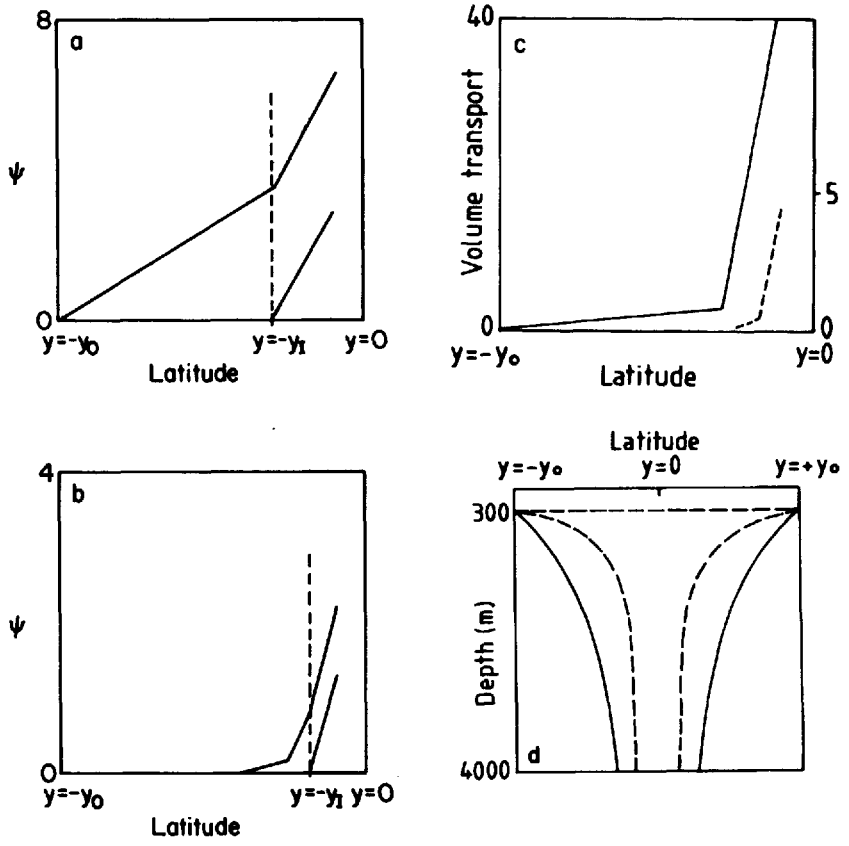

Figure 7. (a) Streamfunction ψ at depths of 150 m (upper line) and 3000 m (lower line) when $N^2 = g'\delta(z + H_M)$ corresponding to a two-density layer ocean. ψ has been nondimensionalized by $\beta y_0/\lambda^2$ where λ^{-1} is the baroclinic Rossby radius $(g'H_M)^{1/2}/f_0$. For this solution, $H_M = 300$ m, $H_1 = 300$ m, the ocean depth $H = 4000$ m, $g' = 0.027\text{m s}^{-2}$ and f_0 and β are chosen appropriate to latitude 40°. $y = -y_1$ marks the latitude where the "bowl" intersects the ocean floor. For $|y| > y_1$ $\alpha = 0.8$ (Eq. (39)). In the region $|y| < y_1$ $\alpha = 0$ and B^2 is chosen so that the velocity in the surface layer is 0.25 m s^{-1} [cf. Eq. (49)]. The solution for the subpolar gyre ($0 < y < y_0$) is obtained by symmetry about $y = 0$. (b) As for (a) except that now $H_1 = 2000$ m and N^2 has a uniform value of 2.5×10^{-3} s^{-1} for -2000 m $< z < -300$ m and is zero otherwise. (c) The vertically integrated volume transport in the western boundary layer (cf Fig. 1). The solid line is for the case shown in Figure 7a and the dashed line for that in Figure 7b. The scale on the left, for the solid line, is in units of $\beta y_0 g' H_M^2/f_0^2$, that on the right, for the dashed line, in units of $\beta y_0 N_1^2 H_1^3/6f_0^2$. The scales have been chosen so that dimensionally the two lines can be compared directly. Note the sudden increase in transport associated with the enhanced barotropic circulation in the region $|y| < y_1$ and the sensitivity to the basic stratification with much greater transport in the two-layer case. (d) The depth D to which the circulation penetrates. Notice how for the two-layer model (solid line) this depth is deeper than for the case shown in (b) (dashed line) for which N^2 has a uniform value over the depth range -2000 m $< z < -300$ m and is zero otherwise.

9. Calculated solutions

Figure 7a,b shows plots of the streamfunction ψ at 150 m and 3000 m depth in two cases with different profiles for the buoyancy frequency N. In Figure 7a, $N^2 = g'\delta(z + H_M)$ so that the solution shown is the same as for a two-layer model in which all the stratification is confined at the base of the WFL. In Figure 7b, on the other hand, N takes a uniform value between $z = -H_M$ and $z = -H_1$, but is zero otherwise. These solutions are calculated using the formulae derived in Sections 5, 6 and 7—that is with the relative vorticity term in (19) neglected. This means that ψ is a function of latitude only at each depth. It has been assumed that in the region $0 < |y| < y_I$, where the ocean floor is playing a role, A^2 is zero, although it is nonzero outside this region. This is equivalent to assuming that within the WFL, the eddies are much more efficient in homogenizing potential vorticity in the intense, barotropically enhanced recirculation area than they are outside. We can see that this assumption is consistent with the behavior of the numerical model shown in Figure 2 by looking at the plot of potential vorticity at depth 150 m.

Looking at Figure 2 we can see that the presence of the eastward jet at mid-basin distinguishes the "time-mean" flow in the western part of the basin from that farther east. Comparing with Figure 7, we see that the solutions found here have features in common with the flow in the western part. Note the sudden increase in westward velocity that is associated with the enhanced barotropic circulation in the region $|y| < y_I$ indicated by the sudden increase in the gradient of ψ. A corresponding increase is found in the model at the boundary of the deep recirculation flanking the eastward jet (marked by the arrows in Fig. 2). Note also that a sudden increase in westward velocity between 35N and 36N is found in the observations described by Schmitz (1980) and shown in Figure 3b. Furthermore, the enhanced barotropic circulation found here clearly leads to a deep circulation reminiscent of Worthington's (1976) proposed deep recirculation for the Gulf Stream system (see Fig. 3a). In connection with this, Figure 7c shows the vertically integrated transport in the western boundary layer, showing an increase with latitude for the subtropical gyre similar to that observed for the Gulf Stream system (see Fig. 1).

Comparing Figure 7a with Figure 7b, we can see that the flow field outside the region of enhanced barotropic circulation is strongly dependent on the choice made for N. In the case for which N is uniform in the region $-H_1 < z < -H_M$, the velocities are very weak in this region and only start to increase once the depth D of the "bowl" increases rapidly near $y = \pm y_I$ (see Fig. 7d). This dependence on the choice for N is not surprising when one looks at Eq. (29) and notes that ψ depends on the integral of N^2 upward from depth D. Clearly, such weak velocities suggest that in the outer parts of the two gyre system (i.e. away from $|y| = y_I$), Sverdrup dynamics (not included in the lowest order solutions given here—see Section 3 and Appendix 2) will play an important role. This has, in fact, been suggested by Greatbatch (1986) on the basis of

dynamical considerations which arise once we move away from the "inertial," "almost-free" limit. This was also found to be the case in the eddy-resolving calculation of Robinson *et al.* (1977)—see their Figure 9a. It is also supported by the fact that the calculated Sverdrup transport for the Gulf Stream at 31N is 32 Sverdrups (Leetmaa and Bunker (1978)) which compares well with the observed transport of 32 Sverdrups through the Florida Straits (Richardson *et al.* (1969)).

Related to the difference in ψ between the two cases is the difference between the depths D shown in Figure 7d. This difference arises because of the dependence of D on ψ_M in Eq. (34). For the two-layer stratification ψ_M is much greater outside $|y| = y_I$ so that D is correspondingly deeper. This figure also shows clearly how the latitudinal extent of the circulation shrinks with depth toward mid-basin, $y = 0$. This is also a feature of the numerical model results shown in Figure 2.

10. Summary and discussion

We have seen how, by allowing a model ocean to have a memory of its potential vorticity, approximate solutions can be obtained analytically which exhibit a deep westward recirculation resembling that proposed by Worthington (1976) for the Gulf stream system. We noted in Section 5 that the key to setting up the solutions is the highly nonlinear, swift, western boundary current which carries its potential vorticity toward mid-basin and leads to the formation of the eastward jet which penetrates into the interior, as in eddy-resolving numerical models (see Holland *et al.*, 1983, for a review). By carrying low potential vorticity northward (subtropical gyre) the circulation is stretched downward until it intersects the ocean floor. The presence of the ocean floor then requires there to be an enhanced barotropic circulation of the gyre. This is driven by eddies and dissipated by bottom friction. It is this enhanced barotropic circulation which we have compared with Worthington's deep recirculation. It should be noted that in this model, the baroclinic structure of the gyre provides a window within which this enhanced barotropic circulation takes place. In particular, the north-south scale of the deep recirculation is set by the baroclinic structure of the gyre.

The approximation made to obtain these solutions has been to neglect the relative vorticity in the gyre interiors. We can use (53) to check the consistency of this approximation. It is apparent that wherever the solutions we have found vary on a scale comparable to or less than $(-u_I/\beta)^{1/2}$ they are likely to be modified by the neglected relative vorticity term. This will be the case where the "bowl" deepens rapidly and intersects the ocean floor. Since the relative vorticity calculated from our solutions is positive (subtropical gyre) in this region, we can expect this term to cause the "bowl" to deepen even more rapidly than we have found here and broaden the region occupied by the deep recirculation. This is because positive $\nabla^2\psi$ can partly balance the negative βy

term in (19). Also when the width of the deep recirculation region λ_I is itself comparable to $(-u_I/\beta)^{1/2}$, the relative vorticity can be expected to modify the structure of the deep recirculation region itself. These points will be explored in a later paper. However, preliminary results suggest that the velocity within the deep recirculation region cannot increase ad infinitum as B^2 decreases (and hence the boundary layer width increases) as suggested by (49). Furthermore, as $B^2 \to 0$, i.e. as the potential vorticity in the bottom layer becomes more homogeneous, then so the vertical shear in the westward flow is reduced (the model of Robinson *et al.* (1977), for example, exhibits very little shear in this flow). Taking $u_I = 0.25$ m s^{-1}, appropriate for the model shown in Figure 2, gives $(u_I/\beta)^{1/2} = 112$ km. This is sufficiently large compared to the width of the deep recirculation (approx. 420 km) to suggest that the relative vorticity is playing some role in this region.

It is not proposed here to enter into a detailed comparison between the "time-mean" circulation in eddy-resolving numerical models and the solutions we have found (it is hoped to do this in a later paper). An obvious point of discrepancy, however, concerns the zonal penetration of the eastward jet. For the solutions found here, this jet extends all the way to the eastern boundary. This contrasts with the situation found in models (see Fig. 2). However, the solutions we have found apply in the "inertial," "almost-free" limit in which potential vorticity is exactly conserved following the flow. As we move away from this limit, we expect the eddies to become increasingly effective in removing relative vorticity from the jet and in confining it more and more to the western part of the basin. This is the situation found by Holland and Schmitz (1985). By considering a number of different experiments with multi-level eddy-resolving numerical models they concluded that the zonal penetration scale of the eastward jet depends on a balance between instability processes that tend to confine it near to the western boundary and inertial processes that try to extend it all the way to the eastern boundary. A similar situation was also found by Greatbatch and Yamagata (1985) in an equatorial example. Here, advection of relative vorticity from the western boundary was important for maintaining a steady state eastward jet along the equator. The jet was found to extend progressively eastward as the lateral mixing co-efficient (of momentum in this case) was reduced. The question of this zonal penetration is further discussed in Greatbatch (1987).

Acknowledgments. I am most grateful to Toshio Yamagata who first interested me in the idea of the "inertial," "almost-free" limit. Peter Killworth, John Huthnance and two anonymous referees provided helpful comments on the manuscript. Conversations with John Marshall and George Nurser during the early stages of this work are acknowledged. Funding came from the Natural Environmental Research Council of the U.K., the award of a University of Liverpool Research Fellowship and grant No A1397 from the Natural Sciences and Engineering Research Council of Canada. The hospitality of the Department of Applied Mathematics and Theoretical Physics at the University of Liverpool was much appreciated. This is contribution number 137 of the Newfoundland Institute for Cold Ocean Science.

APPENDIX 1

Comparison with the hydrographic section along 50°W made by *"Atlantis"* in 1956.

The purpose of this appendix is to compare the depth D of penetration of the circulation as estimated using the theory in this paper with that which can be deduced from the *Atlantis* section. This latter is taken to be given by the heavy black line in Figure 8 which roughly marks the boundary of the region within which potential

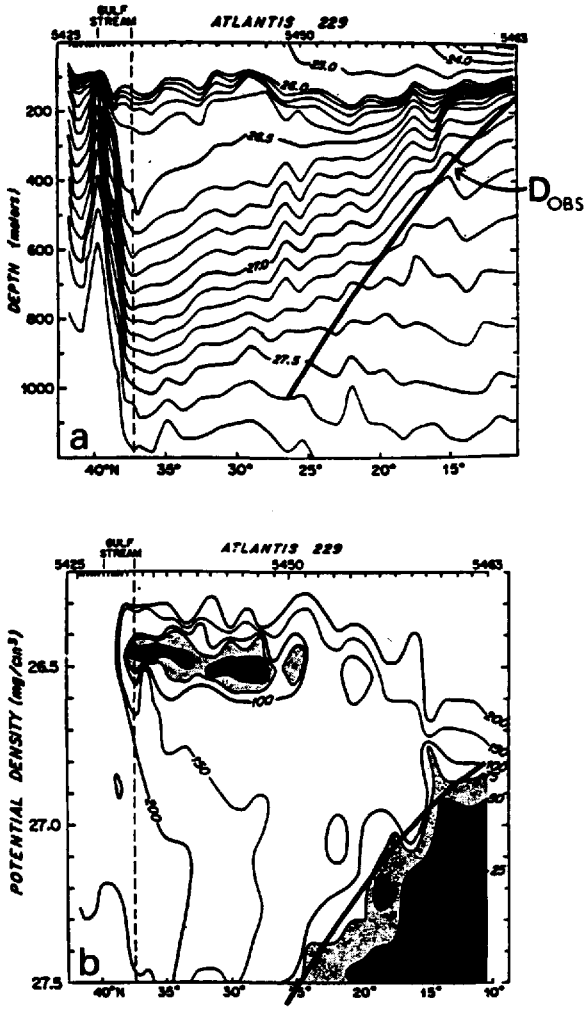

Figure 8. Property sections along 50W made by *Atlantis* in 1956. (a) shows potential density and (b) potential vorticity plotted with potential density as ordinate. Shading emphasizes low potential vorticity water masses. The heavy black line marks the depth D_{OBS} (see Appendix 1) (from McCartney, 1982).

Table 1. A comparison between depth D as given by (55) and D_{OBS} (see text). Depths in meters.

latitude	10°	15°	20°	25°	30°	35°
D	169	261	687	1055	1920	4338
D_{OBS}	169	300	600	929	—	—

vorticity q has been homogenized along the isopycnal surfaces. The depth of this line, labelled D_{OBS}, is given for various latitudes in Table 1.

To obtain a theoretical estimate for D_{OBS} we must repeat the analysis at the beginning of Section 5 this time without making the quasi-geostrophic approximation. We do, however, assume that there is a basic density field $\rho = \bar{\rho}(z)$ which the ocean would have if it were undisturbed and at rest, as is done in quasi-geostrophic theory. This sets the undisturbed spacing of the isopycnals corresponding to a state of zero vortex stretching. Below those layers exposed to surface forcing and above the influence of the ocean floor, the effect of eddies is to homogenize q along isopycnal surfaces. We assume, as we did before, that isopycnals in this region have their undisturbed spacing at the latitude of the zero wind stress curl line θ_0 (this was $y = 0$ before and corresponds to the choice $c_0(z) = 0$ for $-H < z < -H_M$ in (21)). Within the homogenized region we therefore have

$$q = \frac{f}{\rho_0}\frac{\partial \rho}{\partial z} = \frac{f_0}{\rho_0}\frac{\partial \bar{\rho}}{\partial z}. \tag{54}$$

Here ρ is density, the Coriolis parameter $f = 2\Omega\sin\theta$, where θ is latitude, and $f_0 = 2\Omega\sin(\theta_0)$. Putting $\partial\bar{\rho}/\partial z = \mu$, (54) can be written as

$$\partial\rho/\partial z = \frac{\sin\theta_0}{\sin\theta}\mu(\rho).$$

It then follows that assuming we know the depth h of an isopycnal of density $\rho = \rho_1$, say, which passes through the homogenized region, the depth $-z$ (z is measured positive upward with $z = 0$ at the surface) of an isopycnal of density $\rho > \rho_1$ is given by

$$-z = h - (\sin\theta/\sin\theta_0)\int_{\rho_1}^{\rho}\frac{1}{\mu(\rho)}\,d\rho.$$

Now the edge of the "bowl" containing the circulation, which is the surface $z = -D(\theta)$, occurs when this depth $-z$ is equal to the depth the isopycnal has in the undisturbed ocean outside the "bowl" where $\rho = \bar{\rho}$(cf. (24)). This means that D is given by both

$$D = h - \frac{\sin\theta}{\sin\theta_0}\int_{\rho_1}^{\rho}\frac{1}{\mu(\rho)}\,d\rho$$

and

$$D = H_M - \int_{\rho_1}^{\rho} \frac{1}{\mu(\rho)}\, d\rho$$

from which the integral can be eliminated to give

$$D = \frac{1}{\left\{1 - \dfrac{\sin\theta}{\sin\theta_0}\right\}} \left\{h - \frac{\sin\theta}{\sin\theta_0} H_M\right\}. \tag{55}$$

Here H_M is the depth the isopycnal $\rho = \rho_1$ has in the undisturbed ocean. This equation corresponds to Eq. (31) and like that equation does not depend explicitly on the basic density field $\bar{\rho}(z)$.

Table 1 shows values of D calculated using (55) with h taken to be the depth of the $\sigma_\theta = 26.8$ isopycnal in the *Atlantis* section (Fig. 8). H_M is taken to be the depth of this isopycnal at 10N and θ_0 is taken to be 40N. The agreement with D_{OBS} is clearly quite good. Notice how D rapidly deepens north of about 30N and note also that the solid line in Fig. 8 (which defines $z = -D_{\text{OBS}}$) curves down toward the Gulf Stream in the same way as does D defined by Eq. (34) and shown in Figure 6 for the case when $A^2 = 0$. (A proper test of the theory would be to use it to calculate h. This, however, would clearly require a detailed analysis of surface processes which is beyond the scope of this paper. The fact, however, that D (and D_{OBS}) curves downward in a way similar to that shown in Figure 6 is a consequence of the similarity between h and the displacement of the isopycnal at the base of the WFL i.e. at $z = -H_M$ in that figure. In the theory, this displacement is dependent on the assumption that the flow in the surface layer is described, at lowest order, by the "inertial" "almost-free" limit.)

Finally, we can now calculate the implied basic density gradient which was assumed in the above analysis (although was not needed to evaluate D from (55)). Looking at Figure 8, we can see that the solid curve intersects the $\sigma_\theta = 27.2$ surface at 20N at a depth of 600 m and the $\sigma_\theta = 27.5$ surface at 25N at a depth of 930 m. This implies that a local $\partial\bar{\rho}/\partial z$ of $(27.2 - 27.5)/330 = -9 \times 10^{-4}$ Kgs m^{-4}. However, within the homogenized region (cf. Eq. (54)).

$$q = \frac{f_0}{\rho_0}\frac{\partial\bar{\rho}}{\partial z} \simeq 150 \times 10^{-12}\text{m}^{-1}\text{s}^{-1}$$

which implies $\partial\bar{\rho}/\partial z = 16 \times 10^{-4}$ Kgs m^{-4}, which is almost a factor of 2 larger! This clearly shows that the assumption that a basic density field $\bar{\rho}(z)$ exists is suspect, which perhaps is not very surprising (we can see in Figure 8 that in fact the isopycnals tend to fan-out outside the "bowl" in association with the low q in the tropical zone noted by McCartney (1982)—this, at least, is consistent with the discrepancy found above).

APPENDIX 2

The Sverdrup transport as a first order correction

The governing equation for the steady, "time-mean" circulation is Eq. (8) i.e.

$$J(\psi, q) = \epsilon G \tag{56}$$

where

$$q = \nabla^2\psi + \beta y + \frac{\partial}{\partial z}\left\{\frac{f_0^2}{N^2}\frac{\partial \psi}{\partial z}\right\}$$

and ϵ is a parameter which, for the time being, need not be small compared with 1. In the interior of the gyres, we neglected the contribution of the relative vorticity $\nabla^2\psi$ to q so that (56) becomes

$$J(\psi, \beta y) + J\left(\psi, \frac{\partial}{\partial z}\left\{\frac{f_0^2}{N^2}\frac{\partial \psi}{\partial z}\right\}\right) = \epsilon G. \tag{57}$$

Integrating (57) over the depth of the ocean, the stretching term drops out (using integration by parts and the boundary conditions (24), (25) and (26)) to leave

$$\beta\overline{\psi}_x = \epsilon\overline{G} \tag{58}$$

where

$$\overline{\psi} = \int_{-H}^{0} \psi dz \text{ and } \overline{G} = \int_{-H}^{0} G dz.$$

For the calculations described in this paper,

$$\epsilon G = \frac{F_1(z)}{\rho_0 H_M}\left\{\frac{\partial}{\partial x}(\tau_y) - \frac{\partial}{\partial y}(\tau_x)\right\} - F_2\gamma\nabla^2\psi + \nabla(K\nabla q)$$

where

$$F_1(z) = \begin{cases} 1 & (-H_M \le z \le 0) \\ 0 & \text{(otherwise)} \end{cases}$$

and

$$F_2(z) = \begin{cases} 1 & (-H \le z \le -H_1) \\ 0 & \text{(otherwise).} \end{cases}$$

Here (τ_x, τ_y) is the surface wind stress, γ is the bottom friction coefficient and $\nabla \cdot (K\nabla q)$ is the eddy flux divergence term parameterized as a down-gradient transfer $(K > 0)$.

When the surface wind stress curl dominates ϵG, (58) becomes

$$\beta\bar{\psi}_x = \left\{\frac{\partial}{\partial x}(\tau_y) - \frac{\partial}{\partial y}(\tau_x)\right\}\Big/\rho_0 \tag{59}$$

which is just the classical Sverdrup relation.

The "inertial," "almost-free" limit is precisely the limit in which $\epsilon \to 0$. (Clearly we need to nondimensionalize (56) in an appropriate way so that ϵ arises naturally as a small parameter. The reader is referred to Niiler (1966) to see how this works for the barotropic model. A similar procedure would be used here.) Eq. (58) is then dominated by an x-independent solution—the solutions for the gyre interiors found in Sections 5 and 7 of this paper (see also the discussion in Greatbatch (1986) of his Eq. (7) to which (59) corresponds). Let us, however, consider the expansion in terms of ϵ discussed in Section 2. At lowest order we have Eq. (9) i.e. $J(\psi_0, q_0) = 0$ and at next order equation (12) i.e.

$$J\left(\psi_0, q_1 - \frac{\partial Q}{\partial \psi_0}(\psi_0, z)\psi_1\right) = G_0 \tag{60}$$

where

$$G_0 = \frac{F_1(z)}{\rho_0 H_M}\left\{\frac{\partial}{\partial x}(\tau)_y - \frac{\partial}{\partial y}(\tau_x)\right\} - F_2\gamma\nabla^2\psi_0 + \nabla\cdot(K\nabla q_0). \tag{61}$$

As before, we neglect the relative vorticity contribution to the potential vorticity. Then

$$q_1 = \frac{\partial}{\partial z}\left\{\frac{f_0^2}{N^2}\frac{\partial \psi_1}{\partial z}\right\}$$

$$\frac{\partial Q}{\partial \psi_0}(\psi_0, z) = c_1(z) \qquad (c_1 \text{ given by (20)})$$

and

$$\beta y + \frac{\partial}{\partial z}\left\{\frac{f_0^2}{N^2}\frac{\partial \psi_0}{\partial z}\right\} = c_1(z)\psi_0 + c_0(z) \qquad (c_0(z) \text{ given by (21)})$$

so that using integration by parts and the boundary conditions (24), (25) and (26), we see that integrating (60) over the depth of the ocean leads to

$$\beta(\bar{\psi}_1)_x = \bar{G}_0 \tag{62}$$

where

$$\bar{\psi}_1 = \int_{-H}^{0}\psi_1\,dz \quad \text{and} \quad \bar{G}_0 = \int_{-H}^{0} G_0\,dz.$$

This shows that the dynamics represented by Eq. (58) enters at first order when we work in the "inertial" "almost-free" limit (i.e. $\epsilon \ll 1$). When the wind stress curl term dominates G_0, Eq. (62) is just the classical Sverdrup relation. This shows that Sverdrup dynamics is a first order correction to the solutions for the gyre interiors found in this paper.

It is also easy to see how we can calculate the vertical distribution of the transport associated with the first order correction. Neglecting the relative vorticity $\nabla^2\psi$, as before, Eq. (60) takes the form

$$U\frac{\partial}{\partial x}\left\{-\frac{1}{H_M}\frac{f_0^2}{N^2}\frac{\partial\psi_1}{\partial z}\bigg|_{z=-H_M} + A^2\psi_1\right\} = G_M \tag{63}$$

in the depth range $-H_M \le z \le 0$.

$$\frac{\partial}{\partial x}\left\{\frac{\partial}{\partial z}\left\{\frac{f_0^2}{N^2}\frac{\partial\psi_1}{\partial z}\right\}\right\} = 0 \tag{64}$$

in the depth range $-H_1 < z < -H_M$, and

$$U_B\frac{\partial}{\partial x}\left\{\frac{1}{(H-H_1)}\frac{f_0^2}{N^2}\frac{\partial\psi_1}{\partial z}\bigg|_{z=-H_1} - B^2\psi_1\right\} = G_B \tag{65}$$

in the depth range $-H \le z \le -H_1$. Here U is given by (49) and U_B is given by evaluating (48) for u in the depth range $-H \le z \le -H_1$. Similarly, G_M and G_B are obtained by evaluating (61) in the appropriate depth ranges. Integrating (64) leads to

$$\frac{f_0^2}{N^2}\frac{\partial \mathrm{v}}{\partial z} = C \tag{66}$$

where v is the northward velocity $(\psi_1)_x$ and C is a function of the horizontal coordinates x and y to be determined. Using (66), (63) and (65) become

$$U\left\{-\frac{C}{H_M} + A^2V_M\right\} = G_M \tag{67}$$

and

$$U_B\left\{\frac{C}{(H-H_1)} - B^2V_B\right\} = G_B \tag{68}$$

where $V_M = (\psi_1)_x$ and $V_B = (\psi_1)_x$ in the appropriate depth ranges. We also have, integrating (66),

$$V_M = C\int_{-H_1}^{-H_M}\frac{N^2}{f_0^2}\,dz + V_B \tag{69}$$

(67), (68) and (69) are three equations for the three unknowns V_M, V_B and C and so can be solved.

REFERENCES

Batchelor, G. K. 1956. On steady laminar flow with closed streamlines at large Reynolds number. J Fluid Mech., *1,* 177–190.

Bower, A. S., H. T. Rossby and J. L. Lillibridge. 1985. The Gulf Stream—barrier or blender? J. Phys. Oceanogr., *15,* 24–32.

Bretherton F. P. and D. B. Haidvogel. 1976. Two-dimensional turbulence above topography. J. Fluid Mech., *78,* 129–154.

Fofonoff N. P. 1954. Steady flow in a frictionless homogeneous ocean. J. Mar. Res. *13,* 254–262.

Gill, A. E. 1971. Ocean models. Philos. Trans. R. Soc. London, Ser. A, *270,* 391–413.

—— 1982. Atmosphere-Ocean Dynamics. Academic Press, NY, 662 pp.

Greatbatch, R. J. 1986. On the "time-mean" circulation in wind-driven, quasi-geostrophic, eddy-resolving ocean general circulation models. Ocean Modelling, *71,* (unpublished manuscript).

—— 1987. On the scaling of inertial subgyres. Dyn. Atmos. Oceans, (submitted).

Greatbatch, R. J. and T. Yamagata. 1985. Fofonoff-type, inertial mode steady states in a model of the equatorial oceans. J. Phys. Oceanogr., *15,* 1349–1354.

Hellerman, S. 1965. Computations of wind stress fields over the Atlantic Ocean. Mon. Wea. Rev., *93,* 239–244.

Holland, W. R., D. E. Harrison and A. J. Semtner, Jr. 1983. Eddy-resolving numerical models of the large-scale ocean circulation, *in* Eddies in Marine Science, A. R. Robinson, ed., Springer-Verlag, Berlin and NY, 379–403.

Holland, W. R., T. Keffer and P. B. Rhines. 1984. Dynamics of the ocean general circulation: the potential vorticity field. Nature, *308,* 698–705.

Holland, W. R. and W. J. Schmitz. 1985. Zonal penetration scale of model midlatitude jets. J. Phys. Oceanogr., *15,* 1859–1875.

Keffer, T. 1985. The ventilation of the world's oceans: maps of the potential vorticity field. J. Phys. Oceanogr., *15,* 509–523.

Knauss, J. A. 1969. A note on the transport of the Gulf Stream. Deep-Sea Res., *16* (suppl.), 117–123.

Leetmaa, A. and A. F. Bunker. 1978. Updated charts of the mean annual wind stress, convergence in the Ekman layers and Sverdrup transports in the North Atlantic. J. Mar. Res., *36,* 311–322.

Luyten, J. R., J. Pedlosky and H. Stommel. 1983. The ventilated thermocline. J. Phys. Oceanogr., *13,* 292–309.

Marshall J. and A. J. G. Nurser. 1986. Steady free circulation in a stratified, quasi-geostrophic ocean. J. Phys. Oceanogr., *16,* 1799–1813.

Marshall, J. and G. Shutts. 1981. A note on rotational and divergent eddy fluxes. J. Phys. Oceanogr., *11,* 1677–1680.

McCartney, M. S. 1982. The subtropical recirculation of mode waters. J. Mar. Res., *40* (suppl.), 427–464.

McDowell, S., P. B. Rhines and T. Keffer. 1982. North Atlantic potential vorticity and its relation to the general circulation. J. Phys. Oceanogr., *12,* 1417–1436.

McWilliams, J. C., W. R. Holland and J. H. S. Chow. 1978. A description of numerical Antarctic circumpolar currents. Dyn. Atmos. Oceans, *2,* 213–291.

Munk, W. H. 1950. On the wind-driven ocean circulation. J. Meteorol., *7,* 79–93.

Niiler, P. 1966. On the theory of wind-driven ocean circulation. Deep-Sea Res., *13,* 597–606.

Niiler, P., A. R. Robinson and S. L. Spiegel. 1965. On the thermally maintained circulation in a closed ocean basin. J. Mar. Res., *23,* 222–230.

Pedlosky, J. 1965. A necessary condition for the existence of an inertial boundary layer in a baroclinic ocean. J. Mar. Res., *23,* 69–72.

Pierrehumbert, R. T. and P. Malguzzi. 1984. Forced coherent structures and local multiple equilibria in a barotropic atmosphere. J. Atmos. Sci., *41,* 246–257.

Rhines, P. B. and W. R. Holland. 1979. A theoretical discussion of eddy-driven mean flows. Dyn. Atmos. Oceans, *3,* 289–325.

Rhines, P. B., W. R. Holland and J. Chow. 1985. Experiments with buoyancy-driven ocean circulation. NCAR Tech. Note #260, NCAR, Boulder, Colorado.

Rhines, P. B. and W. R. Young. 1982a. A theory of wind-driven ocean circulation. 1. Mid-ocean gyres. J. Mar. Res., *40* (suppl.), 559–596.

—— 1982b. Homogenisation of potential vorticity in planetary gyres. J. Fluid Mech., *122,* 347–368.

Richardson, W. S., W. J. Schmitz and P. Niiler. 1969. The velocity structure of the Florida current from the Florida Straits to Cape Fear. Deep-Sea Res., *16* (suppl.), 225–231.

Robinson, A. R. 1965. A three-dimensional model of inertial currents in a variable density ocean. J. Fluid Mech., *21,* 211–223.

Robinson, A. R., D. E. Harrison, Y. Mintz and A. J. Semtner. 1977. Eddies and the general circulation of an idealized oceanic gyre: A wind and thermally driven primitive equation numerical experiment. J. Phys. Oceanogr., *7,* 182–207.

Schmitz, W. J. 1977. On the deep general circulation of the western North Atlantic. J. Mar. Res., *35,* 21–28.

—— 1978. Observations of the vertical distribution of low frequency kinetic energy in the western North Atlantic. J. Mar. Res. *36,* 295–310.

—— 1980. Weakly depth-dependent segments of the North Atlantic circulation. J. Mar. Res., *38,* 111–133.

Stommel, H. 1948. The westward intensification of wind-driven ocean currents. Trans. Amer. Geophys. Union, *29,* 202–206.

Stommel, H., P. Niiler and D. Anati. 1978. Dynamic topography and recirculation of the North Atlantic. J. Mar. Res., *36,* 449–468.

Veronis, G. 1966. Wind-driven ocean circulation. Part 2: Numerical solutions of the non-linear problem. Deep-Sea Res., *13,* 31–55.

Welander, P. 1971. Some exact solutions to the equations describing an ideal fluid thermocline. J. Mar. Res., *29,* 60–68.

Worthington, L. V. 1965. On the shape of the Gulf Stream system. Trans. Amer. Geophys. Union, *46,* 99.

—— 1976. On the North Atlantic Circulation. Johns Hopkins Univ. Press, Baltimore, MD, 110 pp.

Young, W. R. and P. B. Rhines. 1982. A theory of the wind-driven circulation II. Gyres with western boundary layers. J. Mar. Res., *40,* 849–872.

Received: *22 May, 1986;* revised: *21 April, 1987.*